

Article

Assessment of the Sustainability of Fibre-Reinforced Concrete by Considering Both Environmental and Mechanical Properties

Fateme Soltanzadeh ^{1,*} , Ali E. Behbahani ¹, Kasra Hosseinmostofi ¹ and Carlos A. Teixeira ² 

¹ ISISE—Institute for Sustainability and Innovation in Structural Engineering, Department of Civil Engineering, School of Engineering, University of Minho, 4800-058 Guimarães, Portugal; aliedalatbehbahani@gmail.com (A.E.B.); id8645@alunos.uminho.pt (K.H.)

² Centre for the Research and Technology of Agro-Environmental and Biological Sciences (CITAB), Universidade de Trás-os-Montes e Alto Douro (UTAD), 5001-801 Vila Real, Portugal; cafonso@utad.pt

* Correspondence: soltanzadehfaranak@gmail.com

Abstract: The environmental consequences of human activities, e.g., the depletion of non-renewable fuel resources, consumption of natural raw materials, and release of huge amounts of CO₂ into the atmosphere, resulted in new challenges in materials engineering. Based on these challenges, building materials must fulfil not only mechanical performance criteria, but also produce the least environmental impact accompanied by their production. In the present study, the possibility of employing scrap tire recycled steel fibres (RSF) as a substitution to industrial steel fibres (ISF) for developing more sustainable fibre-reinforced concretes was explored by adopting a life-cycle approach, integrated both environmental and mechanical properties. Four different fibre-reinforced self-compacting concretes—FRSCCs—were tailored by means of replacing the ISFs partially/totally (i.e., 0%, 50%, 67%, 100% by mass of) with the recycled ones. The effect of applying various dosages of RSFs on mechanical behavior of FRSCC—namely compressive, flexural, and splitting tensile responses—were evaluated experimentally. The environmental impacts associated with the production of each FRSCC were also assessed through life-cycle analysis. The potentiality of the RSFs to be used as concrete reinforcement with a comparable mechanical performance to that of ISF-reinforced concrete and lower environmental footprint was evaluated through a consolidated environmental and mechanical index (*EM*). In this study, using RSFs instead of industrial fibres for developing FRSCC has provided up to 37% higher *EM* index. The results confirmed the promising prospects for the application of RSFs in developing more eco-efficient and sustainable reinforced concrete.

Keywords: fibre-reinforced self compacting concrete; tire recycled steel fibres; mechanical performance; life cycle analysis; sustainability; waste management



Citation: Soltanzadeh, F.; Behbahani, A.E.; Hosseinmostofi, K.; Teixeira, C.A. Assessment of the Sustainability of Fibre-Reinforced Concrete by Considering Both Environmental and Mechanical Properties. *Sustainability* **2022**, *14*, 6347. <https://doi.org/10.3390/su14106347>

Academic Editor: Constantin Chalioris

Received: 24 April 2022

Accepted: 17 May 2022

Published: 23 May 2022

Publisher's Note: MDPI stays neutral with regard to jurisdictional claims in published maps and institutional affiliations.



Copyright: © 2022 by the authors. Licensee MDPI, Basel, Switzerland. This article is an open access article distributed under the terms and conditions of the Creative Commons Attribution (CC BY) license (<https://creativecommons.org/licenses/by/4.0/>).

1. Introduction

Our global society is facing several environmental challenges, such as impacts of climate change, loss of biodiversity, over-use of natural resources, and environmental and health issues, which all threaten sustainable development. In order to move towards a more sustainable world, the World Sustainable Development Summit approved Agenda 2030 [1] that contains 17 Sustainable Development Goals (SDGs). Waste management plays an important and increasingly significant role (due to its association with environmental and social issues) to achieve every aspect of this Agenda [2]. The waste management sector can reduce its own environmental impacts (caused by the waste treatment) by means of decreasing solid waste generation through prevention, reduction, reuse, and recycling. Additionally, this sector can contribute to other sectors' emission reductions by increasing waste utilization and, consequently, complying with the SDGs [3].

Recently, significant attention has been paid globally for recycling and reusing wastes as a substantial substitute for the materials applied in the construction industry. For instance, Alani et al. (2022) [4] have successfully introduced the Polyethylene Terephthalate

(PET) fibre, which is produced by recycling waste plastic bottles and used to develop ultra-high-performance green concrete. The developed ultra-high-performance concrete, reinforced with PET fibre, can provide adequate flexural and tensile strength properties and offers a comparable ductility with conventional ones. Recycling low-density polyethylene fibres for reinforcing an eco-friendly and sustainable self-compacting concrete (SCC) is another example of reusing wastes for developing structural materials [5]. The incorporation of LDPF, especially in an optimum fibre volume fraction of 2%, has demonstrated an enhancement in flexural strength, and has provided a suitable compressive strength and satisfied workability.

In the past few years, disposal of worn and End of Life Tires (ELTs) has emerged as a critical issue for waste management agencies. This is due to the large quantity of the ELTs produced each year (14 to 17 million tons/year) and the very slow rate of ELTs decomposition (600 years), which causes a serious threat to the environment [6]. This environmental impact can be minimized by implementing a viable alternative for the recycling and reusing of scrap tires. In the construction industry, ELTs are considered as a potential and sustainable alternative to some of the manufactured raw materials, such as rubber crumbs (appropriate as additives or aggregates in concrete production, masonry construction, and road and pavement engineering [7–9]) and textile fibres (utilized as reinforcement materials for the expansive soils [10]). ELTs are also the primary source for recovering steel fibre. Tire recycled steel fibres can be employed in the civil engineering field to produce Fibre-reinforced Concrete (FRC), a promising candidate for both structural and non-structural applications [11–13].

In recent years, there have been some research efforts for sustainable, resource conservative, and recycled alternatives to replace the high cost (700 €/t as the lowest price [14]) commercially available steel fibres with steel fibres originating from the tyre recycling industry, herein designated as Recycled Steel Fibres (RSFs), (with a price range from 50 to 200 €/t [14]) in developing FRC [15]. In fact, production of Industrial Steel Fibres (ISFs) consumes the natural resources and causes an adverse environmental impact of CO₂ emission [16]. Besides the environmental and economic benefits of applying RSFs in the development of FRC, using these types of fibres mitigates the brittleness and potential cracking problem of conventional concrete by improving their toughness and post-cracking resistance [17,18].

Evaluating the bond between RSFs and concrete (by means of the fibre pull-out test) has shown that fibre pullout behavior is affected by two main factors, namely: (i) the amount of attached rubber to the fibre surface; and (ii) the fibre geometry. If the rubber covers a large surface area of the fibre, the pullout strength significantly reduces with the increase of the rubber content. The fibre shape of the embedded length also influences the fibre pullout behavior. Previous studies have shown that the more irregular undulations and twisted embedded lengths there are in the RSFs, the higher the fibre pullout load and the greater the probability of fibre rupture [19,20].

Studies on FRC with RSF implies that it has a comparable mechanical behavior—e.g., compressive and flexural behaviour—to that produced by ISFs [20]. Evaluating the flexural behavior of RSF-reinforced concrete has shown the satisfactory contribution of the RSFs to improving the concrete performance in the post-peak stage [14]. The concretes reinforced with a relatively high dosage of RSFs (e.g., 90 kg/m³) can almost retain the maximum flexural tensile strength that can be obtained using a similar dosage of ISFs, up to the ultimate crack width (3.5 mm, as recorded by Zamanzadeh et al., 2015 [21]). However, the RSFs are not effective in bridging across the surfaces of cracks with relatively small crack widths (from crack initiation up to flexural tensile strength) due to the geometry and surface characteristics of these fibres. Thus, the flexural hardening phase that can be developed in case of the ISF reinforced concretes may not be observed in RSF-reinforced concretes with a similar dosage of fibres.

Many researchers [22–24] have addressed the possible use of several fibre types (of different materials and/or geometry) to take advantage of the synergistic effect of hy-

brid fibres on the enhancement of the mechanical behavior of the concrete. For instance, Soltanzadeh et al. (2016) [25] have employed hybrid ISFs and plastic fibres for the total suppression of the steel stirrups in beams. The plastic fibres have mainly contributed to avoiding early plastic shrinkage cracking and to increase the cohesiveness of the concrete, since the low Young's modulus of these fibres is close to the Young's modulus of concrete in the first hours of hydration (setting hours). Further, the synthetic fibres have collaborated with the ISFs to increase the concrete fracture energy and toughness at harden state. The applied ISFs have the responsibility of improving the shear capacity of the beams. These steel fibres have mainly provided the possibility of developing the concrete structural elements without stirrups. Another research [26,27] has investigated the effect of hybrid fibres—including four types of steel macro-fibres (with differing lengths or geometry) and one type of steel micro-fibre—on the tensile behavior of ultra-high-performance concrete. Depending on the type of macro-fibres, they have primarily governed the overall tensile behavior of the concrete. The micro-fibres in hybrid systems have provided a favourable effect on multiple cracking and, consequently, strain hardening of the concrete.

Recently, the mechanical properties of concrete reinforced with hybrid RSFs (of 0.5–0.9% volume fraction, V_f) and polypropylene synthetic fibres—PPFs—(of 0.1–0.5% V_f) have been investigated [17]. This research demonstrated that using hybrid RSFs and PPFs can provide a synergistic effect on restraining the crack growth and the post-cracking behaviour of concrete. The concrete toughness was also enhanced in the presence of PPFs. This research has suggested that the workability of the RSF-reinforced concrete can be improved by means of using PPFs with V_f up to 66.7%. However, the applied dosage of PPF is very important in developing the hybrid RSF/PPF reinforced concrete, since using more than 0.3% V_f of PPFs (with the total fibre content of 1.0% V_f) weakens the mechanical properties of the concrete—namely, the concrete compressive, splitting tensile, and flexural strengths.

A few studies [15,18,26,27] have investigated the influence of hybrid recycled and industrial steel fibres on the mechanical properties of mortar and concrete. These studies have confirmed the enhancement of the mortar/concrete mechanical behavior using the hybrid recycled/industrial steel fibres compared to that of the mono RSF-reinforced concrete. The better mechanical performance of the mortar/concrete has attributed to the positive effect of using hybrid ISF/RSF on multi-level crack stabilization and crack propagation control. Additionally, results of cost-benefit analysis have proved the promising prospects for application of RSFs in state of ISFs in developing FRC [28]. However, further investigations are still necessary in order to clearly understand the relevant aspects of the mechanical properties of hybrid recycled and industrial steel fibre-reinforced concrete [18], and the environmental impacts of partially/totally replacing ISFs with recycled fibres.

The present research explored the possibility of developing more sustainable FRCs, capable of representing appropriate mechanical properties compared to that of the conventional ones and with a reduced ecological impact through the application of the steel fibres recovered from the ELTs. To this aim, four types of Fibre-reinforced Self-Compacting Concretes (FRSCCs) were formulated by means of partially or totally (i.e., 0%, 50%, 67%, 100% mass of) replacing the ISFs with the recycled fibres. The influence of using RSFs of different dosages on the mechanical properties—namely compressive, splitting tensile, and flexural strengths—and post-cracking behavior of the developed FRSCCs were evaluated and compared. A life cycle assessment (LCA) was performed for quantifying environmental impacts associated with the development of the FRSCCs. Finally, the relationship between the mechanical properties of the FRSCCs (by focusing on flexural behaviour and energy absorption capacity) and their environmental impacts were evaluated by means of adopting a recent life-cycle approach, integrating environmental and mechanical properties. Finally, the eco-mechanical performances of the developed RSF-reinforced concretes were compared with that of the concrete reinforced using ISFs, at each stage of the FRSCC life from cradle to gate. The outcome of the presented work introduced more environmentally friendly and sustainable options for reinforcing concretes.

2. Experimental Program

Based on the goal of the present study, four different types of fibre-reinforced self-compacting concrete–FRSCC–were tailored using either 90 kg/m³ mono industrial steel fibre (ISF) or RSF, and by means of applying 90 kg/m³ hybrid RSF and ISF. The influence of replacing the ISFs with different dosages of recycled fibres (i.e., 0%, 50%, 67%, 100% of ISF mass) on the mechanical behaviour of FRSCC was investigated by means of compressive, flexural, and splitting tensile test, as detailed in the following.

2.1. Materials

The RSFs utilized in the present study for developing the FRSCCs was supplied by a scrap tire processing plant in Portugal. The cryogenic process of waste tyres adopted by the tire RSF company for recycling the steel fibres is composed of the four following stages: (i) first of all, the end of life tires (ELT) are shredded into tire chips at ambient temperature (using shredder, wheel loader, and debader); (ii) the shredded tires are then transferred to the cryochamber and frozen with liquid nitrogen to $-90\text{ }^{\circ}\text{C}$ (tunnel cryogenic); (iii) the fragmented tires are reduced to particles of various sizes using a hammer mill, and (iv) finally, the steel fibres are magnetically separated from the rubber and fluff, dried (by means of classifier screens, magnets, dryer, exhaust system), and packed (conveyors, storage silos).

Pictorial descriptions of the RSF used in this study, illustrated as Figure 1a,b, shows that RSFs are characterised by different diameters, lengths, and shapes. Overall, 100 RSFs were grabbed randomly, and the length and the diameter of each fibre was evaluated. The average diameter of the fibres was measured as 0.38 mm (CoV. 40%). The RSFs had the average length of 33 mm (CoV. 38%), and the mean aspect ratio of 91 (CoV. 40%). The frequency of the fibres with a certain length is represented in Figure 1b.

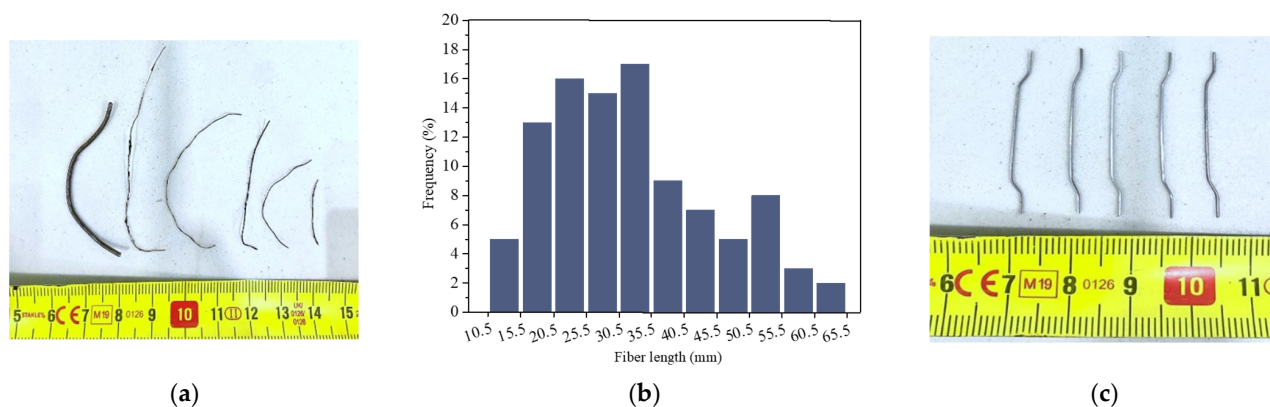


Figure 1. (a) Appearance of unsorted RTSF, and (b) statistical analysis of the RTSF length and (c) 35 mm length ISF.

The density of RSFs were generally considered equal to those of the ISFs (i.e., 7200 kg/m³) in most of the published literature, since the RSFs were assumed free of impurity and tire rubber. Recently, Samarakoon et al. (2019) [29] have evaluated the density of RSFs, finding the same average diameter and length of the RSFs used in the present research, being 3014 kg/m³. This value is almost half of the ISF's density, which refers to a higher number of RSFs in a unit volume of concrete compared to industrial types.

The adopted industrial steel fibres for tailoring the FRSCCs were hooked end steel fibres of 35 mm length, l_f , aspect ratio l_f/d_f of 64 (Figure 1c), and tensile strength of 1395 MPa. The applied cement was CEM I 52.5 R, in accordance with EN 197-1 [30]. The compressive strength of this cement at 3-days and at 28-days were reported by the company as 30 and 52.5 MPa, respectively. Limestone filler, biomass fly ash, a second-generation of superplasticizer based on polycarboxylate ether (PCE) polymers (Glenium SKY 617), tap water, and two types of aggregates (containing river sand and crushed granite with

respectively grain size of 0–2 mm, and 2–12.5 mm) were the rest of material applied for developing the FRSCCs.

2.2. Mix Design Method

The mix design methodology proposed by Soltanzadeh et al. (2015) [31] was adopted for the development of the FRSCCs. This method of developing concrete provides the possibility of tailoring concretes reinforced with high dosages of steel fibres that have rheological and mechanical properties suitable to produce precast/prestressed concrete elements—e.g., self-compacting character—and a relatively high compressive and post-cracking residual strength. Based on this method, a FRSCC with 90 kg/m³ ISF was formulated as a reference concrete. Next, three different types of FRSCC including 90 kg/m³ steel fibres were tailored by means of replacing the ISF at three weight ratios of 50%, 67%, and 100% using RSF.

For developing all the concrete mixes, first, the proportion of constituent materials were evaluated to make an optimized paste. Second, the optimum volume percentage of the aggregates as the granular skeleton of the concrete were assessed, and third, the correlation between the paste and the solid skeleton was optimized. An approximate slump flow [32] of 600 mm was obtained by testing the flowability of all the concrete mixes. All the FRSCCs were designed to pertain to the C50 strength class for a reliable comparison of the concrete mechanical properties at the harden stage.

The adopted compositions of the developed concrete mixes are presented in Table 1 and are nominated by the “FRSCC_{Ri-Ij}” label, where “i” indicates the weight of the RSFs and “j” implies the weight of ISFs applied for developing 1 m³ of the FRSCCs. For instance, the hybrid FRSCC with 45 kg/m³ ISFs and 45 kg/m³ RSFs is identified as “FRSCC_{R45-I45}” in Table 1. Three types of aggregates—two containing fine and coarse river sand with maximum size of 2.4 mm and 4.8 mm, respectively, and one containing crushed granite with 12.5 mm maximum size—were adopted for developing the FRSCCs. The grading curves of the introduced aggregates is illustrated in Figure 2. The concrete compositions were produced using a relatively high dosage of class F fly ash (with 81.15–94.40% particle size of <75 µm and 68.45–85.90% particle size of <45 µm) in order to significantly decrease the friction and the flow resistance of the paste.

Table 1. Concrete compositions (as the material inventory and inputs for each FRSCC considered in the LCA).

Mix ID	C ¹ (kg/m ³)	Fa ² (kg/m ³)	Ls ³ (kg/m ³)	W ⁴ (L/m ³)	Sp ⁵ (L/m ³)	S ⁶ (kg/m ³)	Cs/Ca ⁷ (kg/m ³)	ISF (kg/m ³)	RSF (kg/m ³)
FRSCC _{R0-I90}	500	150	150	214	17	117	621/475	90	-
FRSCC _{R45-I45}	504	200	151	231	18	107	568/435	45	45
FRSCC _{R60-I30}	506	201	152	233	18	113	552/432	30	60
FRSCC _{R90-I0}	511	203	153	235	18	119	535/427	-	90

¹ Cement. ² Fly Ash. ³ Limestone Filler. ⁴ Mixing Water. ⁵ Superplasticizer. ⁶ Fine Sand. ⁷ Coarse Sand. (2–4.75 mm)/Coarse Agg. (4.75–12.5 mm).

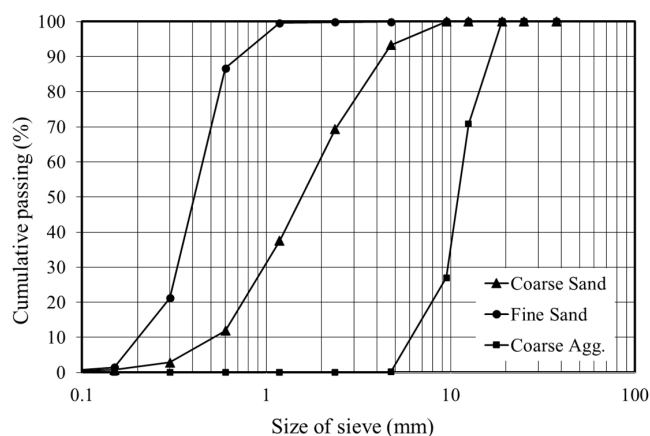


Figure 2. Sieve analysis of the applied aggregates for tailoring the FRSCCs.

Comparison of the concrete compositions, introduced in Table 1, shows that the volume of paste to aggregate ratio was increased in the formulated FRSCCs containing RSFs. In fact, to establish a proper flowability in the tailored concrete reinforced by RSFs—with higher perturbation effect compared to the ISFs—it was necessary to increase the paste/aggregate ratios.

The mechanical performance of the developed FRSCCs were studied in terms of the compressive, flexural, and splitting tensile strength of the hardened concrete at the age of 28 days.

2.3. Compressive and Flexural Behavior

The elastic modulus— E_{cm} [33], and compressive strength— f_{cm} [34], of the tailored FRSCCs were characterized using a total number of twelve cylindrical specimens (three specimens per concrete mix) of 150 mm in diameter and 300 mm in height, as presented in Table 2.

Table 2. Compressive strength and Young's modulus of HPRFC.

Mix ID	f_{cm} ¹ (MPa)	CoV of f_{cm} ² (%)	f_{ck} ³ (MPa)	E_{cm} ⁴ (GPa)	CoV of E_{cm} (%)
FRSCC _{R0-190}	66.10	1.31	58.10	31.41	1.15
FRSCCR ₄₅₋₁₄₅	63.45	1.03	55.54	30.33	1.22
FRSCCR ₆₀₋₁₃₀	63.12	1.27	55.12	30.04	1.15
FRSCCR ₉₀₋₁₀	60.03	1.29	52.03	30.00	1.31

¹ Mean value of compressive strength. ² Coefficient of variation, related to testing of three specimens. ³ Characteristic value of compressive strength. ⁴ Young's modulus.

As it was expected, based on the previous studies [25], the fibre volume fraction did not significantly affect the compressive strength of the tailored FRSCCs. Despite a minor detrimental effect of 100% replacement of ISFs with RSFs, the compressive strengths of all the mixtures reached the target strength of 60 MPa. The marginally higher compressive strength of FRSCC_{R0-190} in comparison with that of FRSCC_{R90-10} can be attributed to the 10% decrease of the coarse aggregate volume and an increase of 9% in the paste volume of the FRSCC_{R90-10} to provide a suitable flowability and avoid the perturbation effect of the 90 kg/m³ RSFs applied to tailor the FRSCC_{R90-10} composition. Reduction in the volume of coarse aggregate, which is regarded as the concrete skeleton, can influence the compressive strength of FRSCC_{R90-10}. The higher perturbation in the skeleton organization of FRSCC_{R90-10} due to the application of the high content of RSFs compared to the other concrete compositions can be another reason for the marginally lower compressive strength obtained by testing FRSCC_{R90-10}.

The flexural behavior of all the developed FRSCCs was evaluated by testing three notched prismatic specimens for each FRSCC, with a 150 × 150 mm² cross-section and 600 mm length under three-point loading conditions, as per RILEM TC 162-TDF [35]. The nominal flexural stress— σ_f , (the $\sigma_f = 1.5PL / (b \times h_{sp}^2)$, (where P is the applied load, and L , b , and h_{sp} are the effective span, width of the specimens, and the depth of the notched cross-section of the specimens, respectively)—versus crack mouth opening displacement (CMOD) relationship of the developed concretes partially/totally reinforced by RSFs were compared with that of the reference concrete FRSCC_{R0-190}, as shown in Figure 3.

For comparison of the energy absorption capacity of each FRSCC, the average σ_f versus midspan horizontal deflection (δ) relationship of the specimens were presented in the same figure (see Figure 3b). Based on RILEM TC 162-TDF [35] recommendations, the energy absorption capacity of the developed FRSCC ($D_{BZ,3Ref}$) was calculated as the area under the load-deflection curve up to the deflection of $\delta_3 = \delta_L + 2.65$ mm, where $\delta_L = 0.05$ mm in the present study.

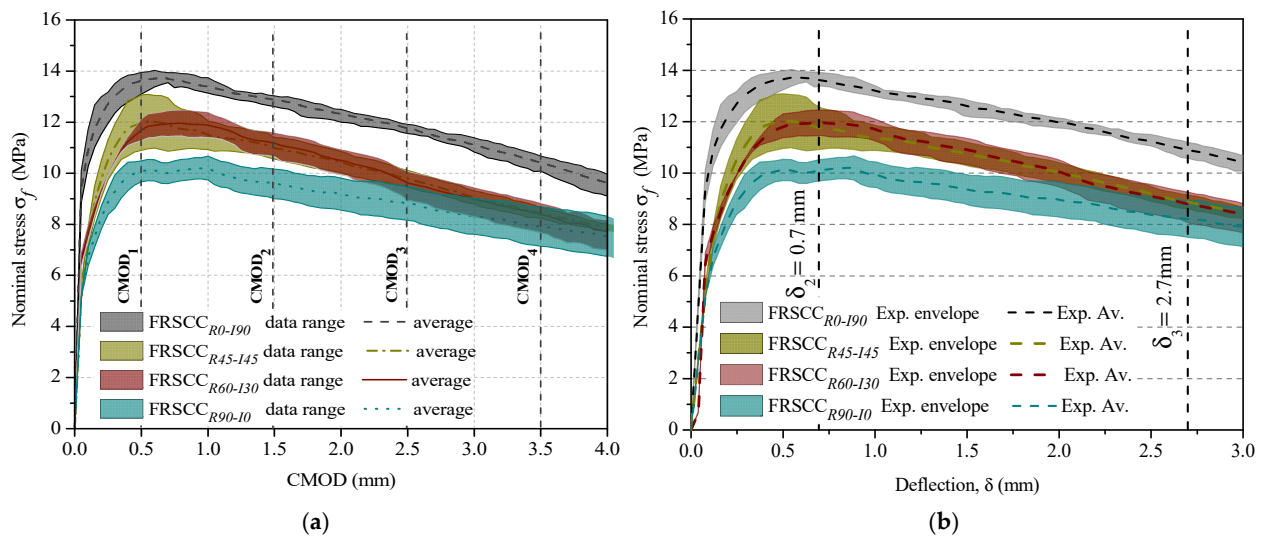


Figure 3. (a) Nominal flexural stress vs. crack mouth opening displacement (CMOD), and (b) nominal flexural stress vs. midspan deflection relationship.

Figure 3 shows that a reduction in the post-cracking flexural behavior and the energy absorption capacity of FRSCC occurred with the increase in the replacement dosage of ISFs by application of RSFs. In fact, after visible crack initiation of the matrix (at about 5 MPa), the ISF reinforcements used for developing the FRSCC_{R0-190} provided the more effective collaboration for increasing the flexural capacity of the concretes, with a higher energy dissipation compared to the RSF used for reinforcing FRSCC_{R90-10}. The longer ISFs in FRSCC_{R0-190} activated as micro-cracks widened, which would have provided a higher degree of macro-crack bridging and fibre-pull-out resistance. The shorter length of the adopted RSFs compared to that of ISFs could be a reason for obtaining the lower post-peak strength, and consequently the lower energy absorption capacity in the concrete specimens totally reinforced with the RSFs (i.e., FRSCC_{R90-10}) compared to that of the reference specimens. In FRSCC, the level of macrocrack bridging and post-crack load sustenance that could be supplied by ISFs of 35 mm length was not provided by the RSFs of a shorter length. However, both types of fibres (i.e., RSF and ISF) provided a ductile post-peak behavior up to 3 mm of CMOD. The residual flexural strength of the reference concrete produced by solely 90 kg/m³ ISFs exceeded 13 MPa up to the crack width of 1.5 mm, whereas the replacement of 45, 60, and 90 kg/m³ of ISFs with recycled fibres in developing the FRSCC caused a 13%, 13%, and 23% reduction, respectively, in the residual flexural strength of these concretes at 1.5 mm CMOD. The calculated $D_{BZ,3Ref}$ for each of the developed concretes are also represented in Table 3.

Table 3. Energy absorption capacity of the developed FRSCC, $D_{BZ,3Ref}$.

	FRSCC _{R0-190}	FRSCC _{R45-145}	FRSCC _{R60-130}	FRSCC _{R90-10}
$D_{BZ,3Ref}$ (Nmm)	92,762	77,967	77,637	68,276

These results suggest that replacing 50%, 67%, and 100% of ISF dosage with the recycled fibres reduced the capacity of absorbing energy to 16%, 16.3%, and 26.4%, respectively. The reduction in the residual flexural strength and the energy dissipation of the FRSCCs produced by using RSFs can be due to the entangled shape of the RSFs applied for replacing the ISFs, which reduced the homogeneity of the fibre dispersion. Additionally, the higher compressive strength of the reference concrete may provide a stronger bond [28] between the fibres and the matrix compared to the fibre/matrix bond in the case of the other tailored FRSCCs. Similarly, the difference between the flexural performance and therefore the

energy absorption capacity of the two FRSCCs—i.e., FRSCC_{R45-145} and FRSCC_{R60-130}—of the same compressive strength was found marginal.

Comparing the density of fibres distributed on the cross-section of the flexural specimens made of FRSCC_{R45-145} and FRSCC_{R60-130} has shown that FRSCC_{R60-130}, tailored by replacing a higher dosage of ISFs with RSFs, was reinforced with a higher total number of fibres. This could be justified by the much lower density of the RSFs compared to that of the industrial fibres. FRSCC_{R60-130}, which contains a higher number of shorter individual RSFs per unit volume of matrix (in comparison to FRSCC_{R45-145}), might provide a longer delay in micro-crack initiation and a more robust crack-bridging at the micro level as a result of the reduced fibre-to-fibre distance in the matrix.

FRSCC_{R45-145} and FRSCC_{R60-130}, reinforced with both hybrid ISFs and RSFs, similarly have shown 18%, 15%, 11%, and 6% higher residual strength, respectively, at the CMOD₁ to CMOD₄ compared to that of the FRSCC_{R90-10} produced solely by means of RSF reinforcements. The improved performance observed by application of hybrid ISFs and RSFs in tailoring FRSCC_{R45-145} and FRSCC_{R60-130} can be attributed to the multi-level crack stabilization and crack propagation control. In fact, compared to FRSCC_{R90-10}, the hybrid FRSCCs containing both shorter (i.e., RSF) and longer (i.e., ISF) fibres in their matrix have provided a more robust crack-bridging at the micro level and a better macro-crack bridging and fibre-pullout resistance at the level of macro-crack.

2.4. Splitting Tensile Behavior

2.4.1. Specimen Preparations and Test Setup

To produce the specimens, a concrete block was cast using each of the four developed FRSCCs from the center point (Figure 4) to provide the possibility of orientating the fibres perpendicular to the radial flow direction. The blocks were measured as 570 × 570 mm² in plan with a 240 mm thickness, as shown in Figure 4a.

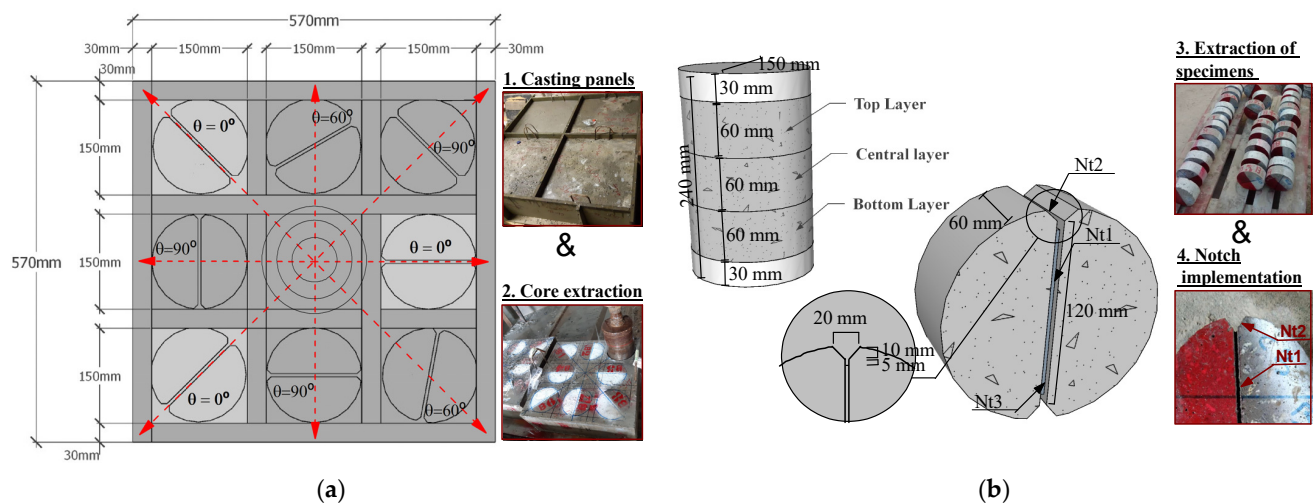


Figure 4. (a) Core extracting plan for splitting tensile test, and (b) cutting of cylinders in $\phi 150 \times 60$ mm specimens and implementation of the respective specimen's notch preparation.

The red arrows in the figure represent the direction of concrete flow during casting. The cast FRSCC blocks were demoulded after three days of being kept in the laboratory environment (with an average temperature of 21 °C and relative humidity of 60%), with the exposed face protected with a plastic film. After 28 days of casting, eight cylindrical cores of 150 mm diameter were drilled out of each concrete block. Three splitting tensile specimens of $\phi 150 \times 60$ mm were produced using each of the extracted cores, as shown in Figure 4b. Two notches of 5 mm depth, named as Nt1 in Figure 4b, were executed on each opposite face of the specimens in order to localize the crack plane. The notched planes

were executed at three different angles of $\theta = 0^\circ$, 60° , and 90° to the direction of concrete flow, as illustrated in Figure 4a.

A total number of nine splitting tensile specimens with the notched plane parallel to the expected concrete flow ($\theta = 0^\circ$) were extracted from each block to evaluate the effect of replacing the ISFs with the recycled fibres on post-cracking behavior of the FRSCC. It is expected that at $\theta = 0^\circ$, the highest number of fibres have located perpendicular to the direction of the notched plane (compared to $\theta = 60^\circ$ or 90°), since it is proven that the fibres are oriented orthogonally to the flux line [36]. The rest of the extracted specimens (with 60° and 90° angle between the notched plane and the direction of the concrete flow) were used for the evaluation of the quantitative relationship between fibre orientation/distribution and the mechanical properties of the developed concrete. Results of the later investigation (i.e., evaluation of fibre orientation/distribution effect on the mechanical behavior of the FRSCC), which are beyond the scope of this article, are not reported in the present work, but the post-cracking behavior of the developing FRSCCs using different dosages of RSF/ISF (with 0° angle between the notched plane and the flow direction) is discussed in the next section.

A schematic representation of the adopted splitting tensile specimens is illustrated in Figure 4b. This figure shows that in addition to the Nt1 notches executed on both surfaces of the specimens, a V-shaped groove with 45° inclination (notch Nt2) was implemented at the extremities of the notched planes in order to induce a stress field corresponding to an almost pure mode I fracture in the notched plane. An additional straight notch of 5 mm depth was presented at the vertices of each V grooves (notch Nt3). This notch assured the crack opening at the notched plane and moved the tip of the crack away from loading points with high stress concentration. All the produced specimens—with the N1 notch direction parallel to the direction of the concrete flow—were categorized in four groups according to the type of the adopted FRSSCs introduced in Table 1.

The splitting tensile test setup was prepared in order to evaluate the relationship of load versus crack width along the fracture surface during the loading process based on the ASTM C-496 [37] standard. The splitting test was conducted in closed-loop displacement control, using an external horizontal linear variable differential transducer (LVDT), positioned on the actuator to control the vertical deformation of the specimen. The load was applied on the top of the N2 notch by means of a 150 kN load cell. The displacement rate of $1.0 \mu\text{m/s}$ was adopted up to the displacement of 2.0 mm. Then, this rate was increased to $2.0 \mu\text{m/s}$ up to the end of the test. An accurate detection and tracking of the crack propagation was carried out using five LVDTs installed on the opposite surfaces (three on the front face and two on the rear face) of each specimen, according to the representation indicated in Figure 5.

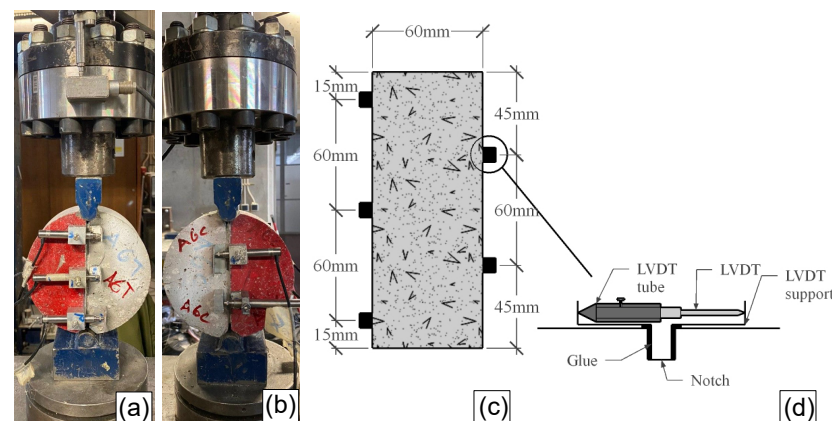


Figure 5. Test setup for splitting tensile tests: (a) specimen front view, (b) back view, and (c) lateral view, and (d) LVDT connection detail.

2.4.2. Results and Discussion

The average and envelope splitting tensile stress ($\sigma_{t,split}$) versus crack mouth opening displacement (CMOD) relationship of all four groups of specimens is illustrated in Figure 6.

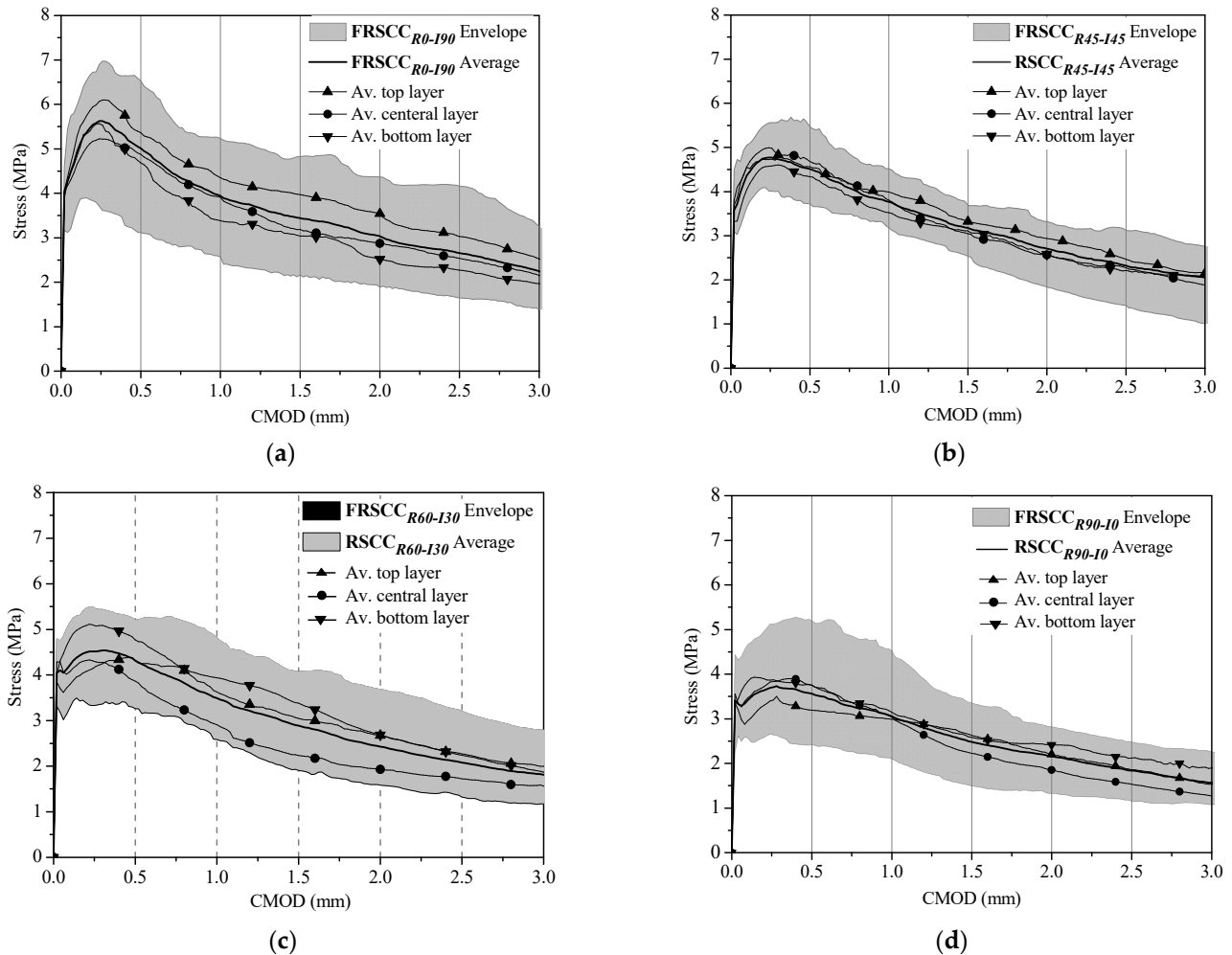


Figure 6. Splitting tensile stress, vs. crack mouth opening displacement (CMOD) of (a) FRSCC_{R0-190}, (b) FRSCC_{R45-145}, (c) FRSCC_{R60-130}, and (d) FRSCC_{R90-10} specimens.

The CMOD was computed as the average of the values measured in the five LVDTs installed in the splitting tensile specimen. The splitting tensile stress was calculated according to Equation (1), as proposed by ASTM C-496 [37].

$$\sigma_{t,split} = \frac{2P'}{\pi ld} \quad (1)$$

where P' is the compressive load applied in the specimen, l is the thickness of the net area in the notched plane (with the nominal values of 50 mm), and h is the diameter of the FRSCC cylinder after executing the notches (equal to 120 mm).

By loading all the specimens, a small load decay was observed after crack initiation, which was followed by a slight strain-hardening branch. Compared to the results of testing the specimens solely reinforced by ISFs, a lower scatter was found in the stress-crack width response of the mono/hybrid RSF-reinforced concrete specimens. The scattering of the results can be attributed to local dispersion and orientation of fibres, as it has already shown by Soltanzadeh et al. (2015) [31]. Counting the number of effective fibres crossing the fracture surface of the specimens has justified a fairly lower scattering of the results in case of mono/hybrid RSF-reinforced specimens, since the opening and propagation of the crack

in case of FRSCC_{R90_I0} (with the number of 250 average effective fibres, N_{eff} , and CoV.9%), FRSCC_{R45_I45} ($N_{eff} = 245$, CoV.9%), and FRSCC_{R60_I30} ($N_{eff} = 241$, CoV.17%) specimens, respectively, were controlled with a much higher number of fibres in comparison to that of the FRSCC_{R0-I90} specimens ($N_{eff} = 174$, Cov.19%).

Figure 6 also compares the average stress–CMOD relationships of the specimens extracted from the top, central, and bottom layer of each FRSCC block (see Figure 4b). The small differences between the results obtained by testing the specimens belonged to different layers indicate that fibre distribution and orientation was not too different along the depth of each concrete block due to the good equilibrium of flowability and viscosity. The average stress–CMOD relationships results of the specimens related to the three layers were found much closer to the $\sigma_{t,split}$ –CMOD relationship obtained by testing all the specimens of a relevant block, in case of the specimens extracted from respectively FRSCC_{R45_I45} and FRSCC_{R90_I0} and FRSCC_{R60_I30} blocks. This could be another reason for obtaining a lower scatter by evaluating the stress–crack width response of the RSF-reinforced concrete specimens in comparison to that of reference specimens.

Despite the relatively high dispersion of the results observed in the case of FRSCC_{R0-I90} specimens, among all the specimens the highest average maximum stress, σ_{max} , and average post-cracking tensile strength was obtained by testing the ISF reinforced specimens. Replacing 50%, 67% and 100% ISFs by the recycled ones in developing FRSCC has reduced the σ_{max} respectively 15%, 19% and 34%. However, a higher average fibre reinforcement density (i.e., ratio of N_{eff} to the specimen's fracture area " A_f ", $D_f = N_{eff}/A_f$) of the mono/hybrid RSF-reinforced concrete specimens ($3.9 \leq D_f \leq 4.2$) compared to that of the specimens made of FRSCC_{R0-I90} ($D_f = 2.8$) offered a more effective resistance to the cracking process and provided a smoother load decay after the peak load. Thus, σ_{max} of FRSCC_{R0-I90} specimens reduced 30% at a crack width of 1 mm, whereas the lower decay of 21%, 23%, and 17% was evaluated for the FRSCC_{R45_I45}, FRSCC_{R60_I30}, and FRSCC_{R90-I0} specimens, respectively, at the same crack width (see Table 4).

Table 4. Maximum and residual stress and dissipated energy due to fracture propagation.

FRSCC		σ_{max}	$\sigma_{0.3}$	$\sigma_{0.5}$	$\sigma_{1.0}$	$\sigma_{1.5}$	$\sigma_{3.0}$	$G_{F0.3}$	$G_{F0.5}$	$G_{F1.0}$	$G_{F1.5}$	$G_{F3.0}$
		(MPa)	(MPa)	(MPa)	(MPa)	(MPa)	(MPa)	(N/mm)	(N/mm)	(N/mm)	(N/mm)	(N/mm)
FRSCC _{R0-I90}	Average	5.63	5.58	5.01	3.94	3.44	2.45	1.49	2.54	4.74	6.58	10.84
	(CoV.)	(19%)	(21%)	(24%)	(25%)	(28%)	(30%)	(17%)	(19%)	(21%)	(22%)	(30%)
FRSCC _{R45-I45}	Average	4.78	4.74	4.51	3.77	3.18	2.05	1.29	2.21	4.26	5.98	9.80
	(CoV.)	(16%)	(15%)	(16%)	(14%)	(14%)	(27%)	(14%)	(15%)	(14%)	(14%)	(15%)
FRSCC _{R60-I30}	Average	4.54	4.54	4.32	3.50	2.89	1.81	1.26	2.15	4.10	5.68	9.10
	(CoV.)	(13%)	(16%)	(16%)	(22%)	(26%)	(26%)	(14%)	(14%)	(15%)	(18%)	(20%)
FRSCC _{R90-I0}	Average	3.73	3.70	3.57	3.06	2.48	1.57	1.03	1.75	3.40	4.78	7.78
	(CoV.)	(23%)	(25%)	(27%)	(27%)	(26%)	(25%)	(22%)	(24%)	(26%)	(26%)	(24%)

This can be attributed to pull-out behavior of the RSFs, which were affected by the geometry of the fibres as well as the amount of rubber attached to the fibre surface. It is already shown [20,38] that RSFs with more irregular and twisted embedded lengths collaborate significantly to provide a higher fibre pull-out load and greater probability of fibre rupture. However, the smooth load decay observed during the post-cracking of the RSF-reinforced concrete specimens has demonstrated that the failure of specimens mostly occurred by the pull-out of the fibres, and the number of broken fibres during the splitting tests was not significant. Regarding the amount of rubber attached to the fibre surface, it should be noted that generally the fibre pull-out strength decreases with the increase of rubber content on the surface of the RSFs [19]. Taking into account that the average stress at crack initiation and the average post-cracking tensile strength have decreased by increasing the replacement dosage of ISF using RSFs, it is possible to derive that some rubber debris attached to the surface of RSFs affected the splitting tensile behavior of the RSF-reinforced concrete. The rubbers caused a lower level of pull-out load for the RSF-reinforced concrete

specimens, which may justify the lower average splitting tensile stress compared to that obtained by testing the reference specimens.

The residual strength parameters (σ_w) and the absorbed energy during the fracture process ($G_{F w}$) at a certain crack width “ w ” (represented by the area under the softening curve up to w) were also computed for all the specimens and presented in Table 4. This table shows the reduction of residual strength and consequently the energy absorbed by increasing the dosage of RSFs in developing the FRSCCs. For instance, the average residual strength obtained by testing the reference specimens at a crack width of 1mm was reduced to 4%, 11%, 23% by replacing 50%, 67%, and 100% ISFs by RSFs, respectively, in developing FRSCC. This reduction in the residual strength led to the relevant absorbed energy being reduced by about 10%, 14%, and 28%, respectively, at $w = 1$ mm. A similar justification has been drawn for the lower stress versus crack opening relationship observed in the case of RSF-reinforced concretes compared to the reference concrete, and can explain the reduction in the residual strength and the respective energy due to fracture propagation at the specific crack width.

To identify the more effective fibres and their best dosage for developing FRSCC, it is of paramount importance to take into account the environmental impact of the developed concrete in addition to the mechanical performances [29,39]. In the present study, an eco-mechanical approach was adopted to evaluate the potentiality of RSFs for replacing the ISFs in tailoring the FRSCCs by considering both environmental and mechanical performances. Therefore, the environmental impacts of the developed concrete were evaluated in the next section through a LCA.

3. Life Cycle Assessment (LCA)

In this study, a LCA was performed, as per the international standards ISO 14040 [40] and ISO 14044 [41], to evaluate the environmental impact of the developed concretes using RSFs and/or ISFs. As previously mentioned, the present research is an attempt to evaluate a novel solution for limiting new material extraction (while retaining the long-term economics of the extracted materials) and reduce the residual waste. A “cradle-to-gate” system boundary was adopted in this study, as the LCA was focused on the circular economy in construction [42,43]. This system boundary included estimating all emissions and energy consumptions by extraction of raw materials (i.e., the cradle), processing (cement, ISF, RSR, fly ash, limestone, sand, superplasticizer, and aggregates), and transporting the materials, and finally mixing the FRSCC compositions (i.e., the gate), as shown in Figure 7. The functional unit was considered as 1 m³ of FRSCC, which is the basis for comparison throughout Sections 3 and 4.

3.1. Life Cycle Inventory

A detailed inventory was created in order to answer the simple question of “how sustainable is the RSF-reinforced concrete throughout its life cycle?”. This phase of LCA, i.e., providing a life cycle inventory, was carried out by means of compilation and quantification of inputs (e.g., energy and materials) and outputs (e.g., emissions and wastes) of the concrete production system, based on the data drives from on-site survey as well as the average data provided by one of the most internationally accredited generic environmental databases [44]. The inventory of the materials considered for developing 1 m³ of each of the formulated FRSCCs is the same as those presented in Table 1. The assigned transportation to each of the introduced materials, as well as the summarized life cycle inventory sourcing, is presented in Table 5.

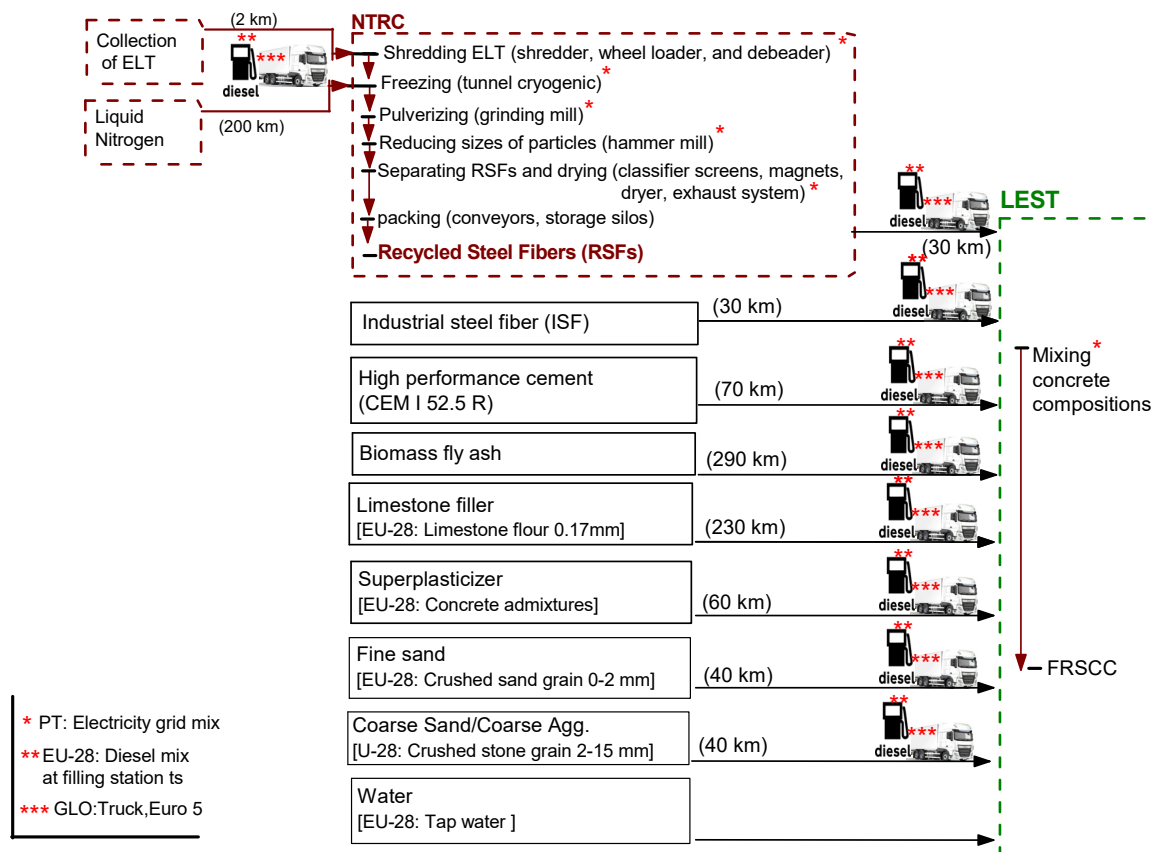


Figure 7. Processes considered in the environmental analysis of the FRSCCs made of RSFs and/or ISFs.

Table 5. LCA source and transportation inputs for FRSCC materials.

Material	Transportation (tkm)				Source
	FRSCCR ₉₀₋₁₀	FRSCC _{R45-145}	FRSCC _{R60-130}	FRSCC _{R90-10}	
Cement	35.00	35.28	35.42	35.77	[45]
Fly Ash	43.50	58.00	58.29	58.87	[44]
Limestone Filler	34.50	34.73	39.96	35.19	[46]
Superplasticizer	1.02	1.08	1.08	1.08	[44]
Fine Sand	4.68	4.28	4.52	4.76	[44]
Coarse Sand + Coarse Agg.	43.84	40.12	38.16	38.48	[44]
RSF	0	1.8	2.4	3.6	Company statements
ISF	3.6	1.8	1.2	0	[47]

For transportation processes, the distances between the places of raw material extraction/storage in Portugal and the concrete mixing plant located at the Laboratory of Structures (LEST), which belongs to the Department of Civil Engineering at the University of Minho, Portugal, was taken into account. The additional details related to the production, procedure, and transportation of the compositions used for tailoring the FRSCC are addressed as follows:

High-performance cement, CEM I 52.5 R, produced at a Portuguese cement plant, was delivered from Porto district, Portugal, to the LEST. The potential environmental impacts of the adopted cement were quantified by considering the inventory listed in the most recent public Environmental Declaration [45] published by the cement plant.

The distance between the cement plant and the LEST was estimated to be 70 km, based on the Google Maps® application. The cement transportation was modeled using a diesel-driven truck of 28–32 t payload capacity (GLO: Truck, Euro 5). The truck was fueled with

diesel using the process “EU-28: Diesel mix at filling stations”. The described choices for the fuel and truck were also set as default option for the limestone filler, fly ash, all types of aggregates, superplasticizer, and industrial/recycled discrete steel fibres.

Biomass fly ash was collected from a biomass co-generation plant in a pulp and paper industry, located in Vila Velha de Ródão municipality, Portugal. The fly ash was considered as a waste, without economic value, and no flows were allocated for its production [40]. Thus, only the impact of transportation from Vila Velha de Ródão to the LEST (290 km distance) was attributed to fly ash.

Industrial Steel Fibres (ISFs) used in the present study was provided by a company located at Porto district in the north of Portugal. Life cycle inventory for the ISF is not available in the GaBi database. Thus, the potential environmental impacts of the applied ISFs were quantified by considering the data presented in the last environmental declaration published by a multinational steel manufacturing corporation [47]. This environmental declaration transparently communicates the environmental performance of the ISFs, though electricity for production was not assigned to a specific country. Therefore, the results of the environmental declaration were advanced in the present work by accounting the electricity grid mixes of Portugal (PT: Electricity grid mix 1–60 kV) in the calculations. The Portuguese energy mix was also set to the default option in LCA of the RSF and mixing the compositions to develop FRSCCs.

Recycled steel fibres (RSFs) were collected from Porto district and transported for 30 km to the LEST. The RSF was produced according to the procedure described in Section 2.1 at a national tire recycling company in the north of Portugal. The process of transporting the end-of-life tires to the municipality was excluded from the system boundaries due to lack of the data in this regard. As the RSFs are the waste material, they do not afford an economic value. Therefore, no flows were allocated to the production of the fibres. Based on the information provided by the company, the company consumes 165.2 kWh electricity to produce 1 ton of its product, including RSFs, rubber granules, and fluffs. To produce 1 ton of the product, the company uses 750 kg liquid nitrogen, which is transported (200 km) to the company by a diesel driven truck of 28–32 t payload capacity. The process of producing RSFs is displayed in a simplified way in Figure 7 within the boundary marked in red color. This process was included in the LCA analysis of the FRSCCs made of hybrid and/or mono RSFs.

The generic data was adopted for life-cycle inventory of the other applied materials—i.e., limestone filler, gravel, sand, water, and superplasticizer—for developing the FRSCCs, as the comparison of different design scenarios for reinforcing the concrete using RSF and/or ISF is of the main goals of the LCA in the present work, and this can be carried out based on this generic/average data [48].

3.2. Impact Assessment

In the impact assessment stage of the LCA, effects of emissions identified and quantified in the inventory for producing one cubic meter (i.e., the functional unit) of each FRSCC are evaluated, in several environmental impact categories (EICs). The emissions are classified into environmental loadings. The environmental loadings are then multiplied by characterization factors to give a single valuation representing the potential effect of the relevant environmental impact category (EIC) on the ecosystem (Equation (2)). Using the EIC indicator facilitates the comparison between environmental impact categories.

$$(EIC\ indicator)_i = \sum_j (E_j \times CF_{i,j}) \quad (2)$$

where $(EIC\ indicator)_i$ stands for the indicator value (per functional unit) for i -th environmental impact category, E_j identifies the release of emission “ j ” (classified under the i -th environmental impact category) per functional unit, and $CF_{i,j}$ is the characterization factor for emission “ j ” contributing to i -th environmental impact category.

In the present study, the environmental impacts were determined with GaBi 6 software, with the possibility of selecting an impact assessment method out of several methods, including the midpoint method “CML 2001” [49]. The impacts were quantified using CML 2001 impact assessment methodology due to the sound scientific basis of this approach, as well as its relatively wide range of emission- and resource-related impact categories available, and the reputation of the CML 2001 method within the scientific community. The environmental performance assessment was carried out based on the following six environmental impact categories from those of the CML 2001 approach, which are easily communicated and representative of the major environmental impact concerns [50–53]: (i) Global Warming Potential, GWP; (ii) Acidification Potential, AP; (iii) Eutrophication Potential, EP; (iv) Abiotic Depletion Potential for Fossil Resources, ADP; (v) Ozone Depletion Potential, ODP; (vi) Photochemical Ozone Creation Potential, POCP.

After calculating the environmental impacts associated with the development of each concrete on the ecosystem, the environmental impact category indexes were weighed and normalized using the following equation [54]:

$$EnScore^k = \sum_{i=1}^6 WNIndex_{i,V_{FS}}^k \quad (3)$$

where $EnScore^k$ is the non-dimensional environmental score for RSF-reinforced concrete alternative k , i is the number of environmental impact category, and $WNIndex_{i,V_{FS}}^k$ is the weighted and normalized score of environmental impact category of i for the alternative k :

$$WNIndex_{i,V_{FS}}^k = \frac{EICIndex_{i,V_{FS}}^k \times \omega_i}{\max\{EICIndex_{i,V_{FS}}^1, EICIndex_{i,V_{FS}}^2, \dots, EICIndex_{i,V_{FS}}^m\}} \quad (4)$$

where $EICIndex_{i,V_{FS}}^k$ is the raw score of an environmental impact category as per functional unit of V_{FS} , ω_i is the importance weight for the impact category i , $m = 3$ is the number of RSF-reinforced concrete alternatives. The symbol $\max\{.\}$ denotes a function identifying the maximum value of the series.

3.3. Interpretation

The quantified values of the potential environmental impacts related to the production of 1 kg of different types of steel fibres applied in developing the FRSCCs, i.e., ISF and RSF, are presented in Table 6. It is evident from the results that the environmental impacts of developing ISFs were much higher, specifically regarding ADP and GWP. These results highlighted the benefits of applying the RSFs in developing a more environmentally friendly concrete.

Table 6. Quantification of the environmental impact categories related to the production of 1 kg of fibre.

Binder	GWP (100 Years)	ODP	AP	EP	POCP	ADP (Fossil Fuels)
	kg CO ₂ eq	kg R11 eq	kg SO ₂ eq	kg PO ₄ eq	kg C ₂ H ₄ eq	MJ eq
RSF	0.0695	2.11×10^{-15}	1.18×10^{-4}	1.97×10^{-5}	3.45×10^{-6}	0.73
ISF	0.771	0.0001	1.05×10^{-3}	3.35×10^{-4}	3.24×10^{-5}	1.01

The environmental impacts of developing 1 m³ of the tailored concretes reinforced by the RSFs and/or ISFs is comparable in Table 7.

Table 7. Environmental impacts of developing 1m³ FRSCCs using RSF and ISF.

Concrete ID	GWP (100 Years)	ODP	AP	EP	POCP	ADP (Fossil Fuels)	EnScore ^k
	kg CO ₂ eq	kg R11 eq	kg SO ₂ eq	kg PO ₄ eq	kg C ₂ H ₄ eq	MJ eq	
FRSCC _{R45_I45}	518	0.009	0.210	0.0613	0.026	1720	1.020
FRSCC _{R45_I45}	491	0.004	0.170	0.0485	0.011	1330	0.779
FRSCC _{R60_I30}	482	0.003	0.156	0.0437	0.006	1190	0.698
FRSCC _{R90_I0}	466	4.53 × 10 ⁻⁹	0.127	0.0343	-0.004	912	0.555

As expected, (by considering the results of analyzing the emissions resulted by producing 1 kg RSF and ISF) tailoring of the reference concrete FRSCC_{R0_I90} (solely reinforced by means of ISFs) caused the development of the highest environmental impacts in all the categories. The environmental impacts of producing FRSCC have reduced by increasing the RSF dosage as the replacement of the ISFs. Thus, the lowest environmental impacts were quantified for FRSCC_{R90_I0} composition. The lowest environmental impact category for the development of FRSCC_{R90_I0} among all the quantified concretes came from the POCP, which was produced due to the relevant transportations. The POCP impact of producing 1 m³ FRSCC_{R90_I0} was quantified as a negative value, because of the NO emissions that occurred during the transportation processes. According to CML 2001, the NO emissions have a negative characterization factor, which caused the transports to appear with negative POCP values.

By comparison, with the FRSCC compositions formulated in the present study (Table 1), it should be noted that the ratio of paste to granular skeleton of the concrete compositions was increased slightly depending on the applied dosage of RSFs (compared to the reference concrete) to provide an almost similar flowability for all the mixes, and to disperse the RSFs uniformly in a concrete mix. Although application of a higher amount of the concrete paste in the case of mono or hybrid RSF-reinforced concretes led to the use of a higher dosage of cement and superplasticizer (which are respectively responsible for the development of the highest proportion of GWP and ADP among all the adopted compositions) [39], the potential environmental impacts of developing these concretes have still decreased. For instance, replacing 50%, 67%, and 100% of the ISFs with the recycled fibers to develop FRSCC reduced GWP impacts by 5%, 7%, and 10%, respectively, in comparison with that of the reference concrete, FRSCC_{R0_I90}. The ADP impact was reduced up to 23%, 31%, and 47% by means of replacing 50%, 67%, and 100% of the ISFs with the RSFs, respectively.

Figure 8 compares the amount of greenhouse gas emissions (i.e., those produced by the development of the concretes reinforced using ISFs and/or RSFs) by representing the breakdown of GWP, one of the highest impact category along the supply chain of concrete production. This figure indicates that the main source of emissions in the reference concrete, FRSCC_{R0_I90}, was associated to the cement application (75%), followed by embodied emissions from production of ISFs (13.4%), and admixture (5.7%), road transport and sand quarrying (both 2.4%), and electricity generation (0.61%). Substituting the relatively high dosage of ISF (i.e., 50%, 67%, and 100% of ISF) by the more sustainable fibres (i.e., RSFs) in developing FRSCC improved the environmental performance of the concretes. The main source of greenhouse gas emissions in the RSF-reinforced concretes was respectively related to application of cement (79% to 85%), admixture production (6.4% to 6.9%), producing ISF and/or recycling scrap tire fibres (1.3% to 7.7%), road transport (2.6% to 2.8%), sand quarrying (2.3% to 2.35%), and electricity generation (0.63% to 0.66%).

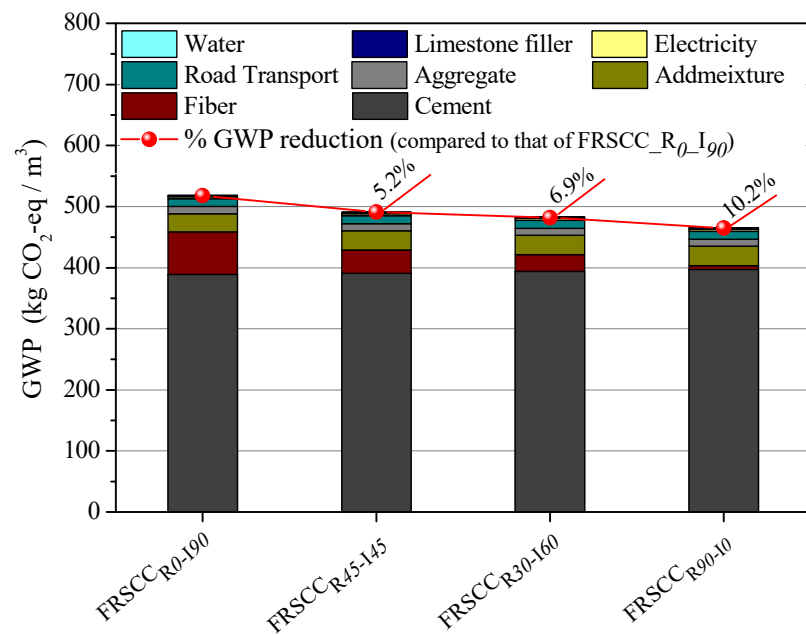


Figure 8. Comparison of GWP impact of developing 1 m³ FRSCC using industrial discrete steel fibres with those developed by recycled tire steel fibres.

Comparison of the results of the environmental score, represented in Table 7 and detailed in Figure 9, has shown that replacing 50%, 67%, and 100% of the ISF with RSF in developing FRSCC reduced the *EnScore*^k up to 24%, 32%, and 46%, respectively. This is due to the share of the weighted and normalized score of all the environmental impacts, *WNIndex*, being reduced by the application of relatively high dosages of RSFs to reinforce the concretes, as shown in Figure 9. The total replacement of ISFs with that of recycled fibres provides the possibility of suppressing the POCP and ADP. The *WNIndex* calculated for ADP, AP, and EP were also reduced up to 47%, 39%, and 44%, respectively, by using FRSCC_{R90_I0} Composition.

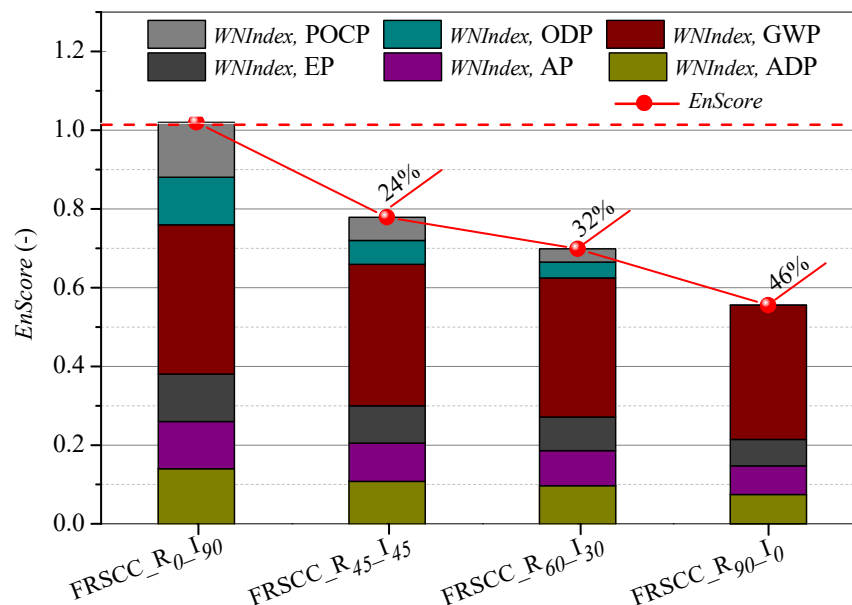


Figure 9. Comparison of the calculations for 1 m³ FRSCC using industrial discrete steel fibres with those developed by recycled tire steel fibres.

In general, replacing the ISFs with the recycled fibres for reinforcing concrete has great potential to produce a FRSCC with lower environmental impacts. However, a trade-off exists between a decreasing environmental impact associated to the reduction of ISF application (see Figure 9) and the consequent decreasing of the mechanical performance of FRSCC (see Figures 3 and 6). Thus, in the next section, the two competing factors of environmental performance and mechanical behavior of the developed FRSCCs is considered simultaneously.

4. Consolidated Environmental and Mechanical Index

In the present section, the simultaneous mechanical and environmental performances of each developed FRSCC (EM^k) were evaluated, based on the formula proposed by Khodabakhshian et al. (2018) [54], as follows:

$$EM^k = \frac{Mec_n^k}{EnScore_n^k} \quad (5)$$

where EM^k is the consolidated index of mechanical and environmental performances of the FRSCC composition alternative k . $EnScore_n^k$ and Mec_n^k are the normalized environmental score and normalized energy absorption capacity of the alternative k , respectively. $EnScore_n^k$ and Mec_n^k can be calculated using Equations (6) and (7), respectively. In these two equations, m is the number of concrete mix alternatives.

$$EnScore_n^k = \frac{EnScore^k}{\max\{EnScore^1, EnScore^2, \dots, EnScore^m\}} \quad (6)$$

$$Mec_n^k = \frac{Mec^k}{\max\{Mec^1, Mec^2, \dots, Mec^m\}} \quad (7)$$

In general, the high tensile/flexural behavior of FRC and its superior ductility and energy absorption capability under bending load make the FRC different from conventional concrete, which is accompanied by brittle failure [55]. Therefore, the ductility-related measurements—such as post-cracking flexural capacity and energy absorption—of the FRC as the most relevant indicators of mechanical performance of fibrous concrete [56–58] are of great importance for the design, construction, and safety evaluation of engineering structures.

Based on the above reasoning, energy absorption capacity, characterized by performing three-point bending test, was selected in this study as the measure of FRSCC mechanical performance. As the energy absorption capacity is one of the most important criteria for the performance evaluation of FRSCC, a similar weight coefficient was considered in the calculation of both the $EnScore_n^k$ and Mec_n^k indexes.

Results and Discussion

The results of evaluating both the normalized environmental and mechanical indexes for all the FRSCCs are presented in Figure 10. From the figure, it is clear that an increase in the substitution dosage of ISFs led to a downward trend of the indexes. The reduction of $EnScore_n$ occurred in a much higher rate in the case of the FRSCCs reinforced with more than 50% RSFs. This shows a superior environmental performance of the concretes tailored by replacing 67% and 100% ISFs with FSRs (i.e., FRSCC_{R90_I0} and FRSCC_{R60_I30}) compared to the rest of FRSCCs. Compared to FRSCC_{R45_I45} composition, FRSCC_{R60_I30} has shown an 8% lower $EnScore_n$, with an almost equal Mec_n index. Thus, replacing 67% of ISFs with recycled fibres can be introduced as the optimum dosage when tailoring a hybrid RSF/ISF-reinforced concrete.

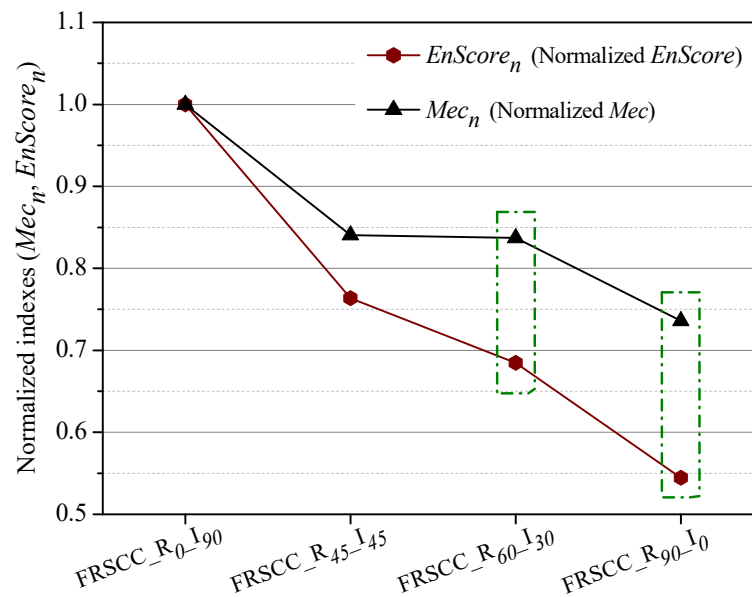


Figure 10. Normalized environmental and mechanical indexes.

The values of consolidated index, EM , for all the concrete compositions are depicted in Figure 11. This figure also introduces the consolidated index values for RSF-reinforced concrete alternative k , by considering each of the environmental categories, EM_{cat}^k , where $cat = GWP, AP, EP, ADP, ODP, POCP$. By considering the results represented in Figure 11a, it is clear that all EM_{cat}^k indexes, with exception of the one related to GWP, were increased by the replacement of ISFs with recycled fibres to reinforce the concretes. The RSF-reinforced concrete compositions, $FRSCC_{R45_I45}$, $FRSCC_{R60_I30}$, and $FRSCC_{R90_I10}$, have shown 16%, 16.3%, and 26% lower energy absorption capacity, respectively, in comparison to that of the reference concrete, $FRSCC_{R0_I90}$. Therefore, a lower normalized mechanical score, Mec_n , was calculated for the RSF-reinforced concretes compared to that of the reference concrete. On the other hand, the reduction in GWP impact by increasing the replacement dosage of ISFs was not as high as that calculated in the case of the other impacts (see Figure 8), since using the RSFs slightly increased the required amount of cement in the development of the FRSCCs (to facilitate the homogeneous dispersion of the fibres). Consequently, the changes in the quantified EM_{GWP} (EM calculated by accounting only GWP impact) for the FRSCCs was marginal.

Although the RSF-reinforced concretes have shown the lower capacity in absorbing energy compared to that of the reference concrete, substitution of ISFs with the recycled ones has still provided an improvement in the consolidated index, EM , of the developed concretes, as shown in Figure 11b. For instance, replacing 100% of the ISFs with the recycled fibres resulted in a 46% reduction in $EnScore_n$, while the normalized mechanical index, Mec_n , was reduced by 26%. Thus, $FRSCC_{R90_I10}$ has shown a 35% higher EM in comparison to that of the reference concrete. Application of 100% RSFs in the development of concrete decreased the major impact of producing FRSCC, related to the extraction of elements and fossil fuels (i.e., ADP), by 47% (see Table 7), and thus provided a 39% increase in EM_{ADP} . Using $FRSCC_{R90_I10}$, the environmental impacts related to AP and EP were reduced up to 40% and 44% (in comparison with the reference concrete), respectively, and led to improve the EM_{AP} and EM_{EP} values by 20% and 32%, respectively. Application of RSFs instead of industrial fibres has also provided the possibility of almost eliminating the ODP and POCP impacts in the production of $FRSCC_{R90_I10}$. The results illustrated in Figure 11 confirm the high eco-mechanical efficiency (the eco-friendlier concrete with acceptable mechanical performances) of the mono/hybrid RSF-reinforced concretes developed in the present study compared to that of the reference concrete produced solely using ISFs. As

forementioned, the FRSCC_{R90-I0} provided the highest consolidated index, EM , among all the FRSCCs, and can be selected as the most eco-mechanical efficient concrete.

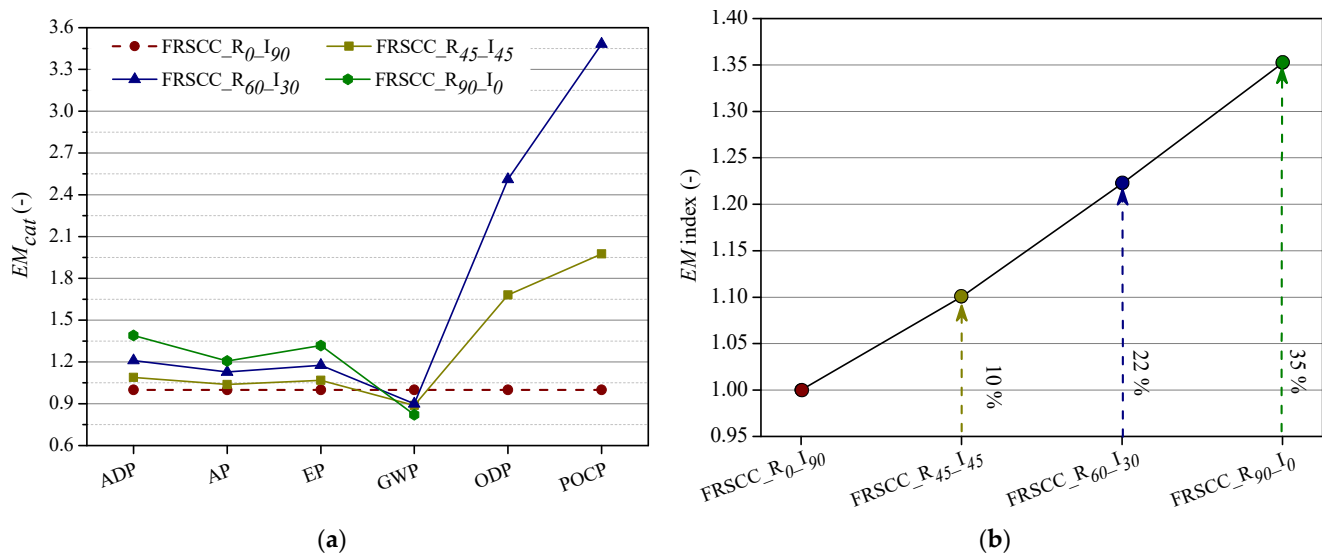


Figure 11. Consolidated index calculated (a) by considering each of the environmental categories (EM_{cat}), and (b) by considering all of the environmental categories (EM index).

5. Conclusions

The present paper evaluates the possibility of recycling high contents of scrap tire steel fibres as the partial/total substitution of ISFs in developing reinforced concrete by taking into account both environmental and mechanical performances. As is evident from the results of the employed analysis, a concrete reinforced by RSFs with a suitable mechanical performance can be deemed as an environmentally lower-damaging concrete. These results contribute to improve the process for the selection of more eco-efficient concrete reinforcement material. The key findings can be summarized as follow:

- Application of ISF and/or RSF did not significantly affect the compressive strength of the tailored FRSCCs. However, increasing the replacement dosage of ISFs by application of RSFs caused a reduction in the post-cracking behavior of FRSCCs in bending and consequently reduced the energy absorption capacity of the concretes. Replacing 50%, 67%, and 100% of ISF dosage with the recycled fibres when developing the FRSCCs reduced the concrete energy absorption capacity to 16%, 16.3%, and 26.4%, respectively.
- Evaluation of the splitting tensile behavior of the FRSCCs showed that replacing 50%, 67%, and 100% of the ISFs by the recycled fibres when developing FRSCC reduced the σ_{max} 15%, 19%, and 34%, respectively. However, a higher D_f in case of mono/hybrid RSF-reinforced concrete specimens ($3.9 \leq D_f \leq 4.2$) compared to that of the specimens made of FRSCC_{R0-I90} ($D_f = 2.8$) offered a more effective resistance to the cracking process, and provided a smoother load decay after the peak load.
- The results of LCA demonstrated that production of RSF led to lower environmental impacts, specifically in the case of the two main impacts: ADP (up to 47%) and GWP (up to 10%), when compared to environmental emissions accompanied by the production of ISF. These results highlighted the benefits of applying the RSFs in developing more environmentally friendly concretes and mortars.
- In order to provide a more reliable and coherent evaluation of the LCA of the developed FRSCCs, an analysis combining mechanical and environmental performance was performed. The results revealed that all the developed mono/hybrid RSF-reinforced concretes could be successfully replaced by the concrete solely reinforced by ISF, resulting in a lower environmental impact and appropriate mechanical behavior. Replacing

50%, 67%, and 100% of ISFs with recycled fibres in the development of concrete can improve the *EM* up to 10%, 22%, and 35%, respectively.

Author Contributions: Conceptualization, A.E.B.; Formal analysis, A.E.B.; Funding acquisition, F.S.; Investigation, F.S., A.E.B. and K.H.; Methodology, F.S. and C.A.T.; Project administration, F.S.; Software, C.A.T.; Supervision, F.S.; Validation, A.E.B. and C.A.T.; Writing—original draft, F.S.; Writing—review & editing, A.E.B. and C.A.T. All authors have read and agreed to the published version of the manuscript.

Funding: The first three authors wish to acknowledge the funding provided by project FOATIDE, reference POCI-01-0145-FEDER-028112, co-financed by the European Regional Development Fund (ERDF), through the Operational Programme for Competitiveness and Internationalization (COMPETE 2020), under Portugal 2020, and by the Fundação para a Ciência e a Tecnologia—FCT (National Agency for Science and Technology). The first author also acknowledges the Scientific Employment funding, No. CEECIND/01627/2017, provided by FCT. The financial support provided by FCT under the project UIDB/04033/2020 is kindly acknowledged by the last author.

Informed Consent Statement: Informed consent was obtained from all subjects involved in the study.

Acknowledgments: The authors thank the collaboration of the following companies: Recipneu—Empresa Nacional De Reciclagem De Pneus, Lda; Secil; BASF Portuguesa S.A.; Celtejo/ALTRI group; PARAPEDRA; RENECAI-Reciclado De Neumáticos De Castilla Y León S.L.; Unibetão, and MOTA-ENGIL.

Conflicts of Interest: The authors declare no conflict of interest.

References

1. United Nations. Technology and the UN 2030 Agenda: United Nations “Technology Facilitation Mechanism” (TFM). 2018. Available online: <https://sustainabledevelopment.un.org/tfm> (accessed on 3 December 2021).
2. IOMC. Chemicals and Waste Management—Essential to Achieving the Sustainable Development Goals (SDGs). Available online: https://www.who.int/iomc/ChemicalsandSDGs_interactive_Feb2018_new.pdf (accessed on 25 January 2022).
3. Marquez, A.J.C.; Filho, P.C.C.; Rutkowski, E.W.; Isaac, R.L. Landfill mining as a strategic tool towards global sustainable development. *J. Clean. Prod.* **2019**, *226*, 1102–1115. [\[CrossRef\]](#)
4. Alani, A.H.; Johari, M.A.M.; Noaman, A.T.; Bunnori, N.M.; Majid, T. Effect of the incorporation of PET fiber and ternary blended binder on the flexural and tensile behaviour of ultra-high performance green concrete. *Constr. Build. Mater.* **2022**, *331*, 127306. [\[CrossRef\]](#)
5. Sor, N.H.; Ali, T.K.M.; Vali, K.S.; Ahmed, H.U.; Faraj, R.H.; Bheel, N.; Mosavi, A. The behavior of sustainable self-compacting concrete reinforced with low-density waste Polyethylene fiber. *Mater. Res. Express* **2022**, *9*, 035501. [\[CrossRef\]](#)
6. Dobrotă, D.; Dobrotă, G.; Dobrescu, T. Improvement of waste tyre recycling technology based on a new tyre markings. *J. Clean. Prod.* **2020**, *260*, 121141. [\[CrossRef\]](#)
7. Ganjian, E.; Khorami, M.; Maghsoudi, A.A. Scrap-tyre-rubber replacement for aggregate and filler in concrete. *Constr. Build. Mater.* **2009**, *23*, 1828–1836. [\[CrossRef\]](#)
8. Al-Fakih, A.; Mohammed, B.S.; Wahab, M.; Liew, M.; Amran, Y.M. Flexural behavior of rubberized concrete interlocking masonry walls under out-of-plane load. *Constr. Build. Mater.* **2020**, *263*, 120661. [\[CrossRef\]](#)
9. Centonze, G.; Leone, M.; Aiello, M. Steel fibres from waste tires as reinforcement in concrete: A mechanical characterization. *Constr. Build. Mater.* **2012**, *36*, 46–57. [\[CrossRef\]](#)
10. Narani, S.S.; Abbaspour, M.; Mir Mohammad Hosseini, S.M.; Aflaki, E.; Moghadas Nejad, F. Sustainable reuse of Waste Tire Textile Fibres (WTTFs) as reinforcement materials for expansive soils: With a special focus on landfill liners/covers. *J. Clean. Prod.* **2020**, *247*, 119151. [\[CrossRef\]](#)
11. Martínez-Barrera, G.; Coz-Díaz, J.J.; Martínez-Cruz, E.; Martínez-López, M.; Ribeiro, M.C.S.; Velasco-Santos, C.; Hagg Lobland Haley, E.; Brostow Witold. Modified recycled tire fibres by gamma radiation and their use on the improvement of polymer concrete. *Constr. Build. Mater.* **2019**, *204*, 327–334. [\[CrossRef\]](#)
12. Graeff, A.G.; Pilakoutas, K.; Neocleous, K.; Peres, M.V.N. Fatigue resistance and cracking mechanism of concrete pavements reinforced with recycled steel fibres recovered from post-consumer tyres. *Eng. Struct.* **2012**, *45*, 385–395. [\[CrossRef\]](#)
13. Yung, W.H.; Yung, L.C.; Hua, L.H. A study of the durability properties of waste tire rubber applied to self-compacting concrete. *Constr. Build. Mater.* **2013**, *41*, 665–672. [\[CrossRef\]](#)
14. Neocleous, K.; Angelakopoulos, H.; Pilakoutas, K.; Guadagnini, M. Fibre-reinforced roller-compacted concrete transport pavements. *Proc. Inst. Civ. Eng. Transp.* **2011**, *164*, 97–109. [\[CrossRef\]](#)
15. Bjegovic, D.; Baricevic, A.; Lakusic, S.; Damjanovic, D.; Duvnjak, I. Positive Interaction of Industrial and Recycled Steel Fibres In Fibre Reinforced Concrete. *J. Civ. Eng. Manag.* **2013**, *19*, S50–S60. [\[CrossRef\]](#)
16. Liew, K.M.; Akbar, A. The recent progress of recycled steel fiber reinforced concrete. *Constr. Build. Mater.* **2020**, *232*, 117232. [\[CrossRef\]](#)

17. Zhong, H.; Zhang, M. Experimental study on engineering properties of concrete reinforced with hybrid recycled tyre steel and polypropylene fibres. *J. Clean. Prod.* **2020**, *259*, 120914. [[CrossRef](#)]
18. Martinelli, E.; Caggiano, A.; Xargay, H. An experimental study on the post-cracking behaviour of Hybrid Industrial/Recycled Steel Fibre-Reinforced Concrete. *Constr. Build. Mater.* **2015**, *94*, 290–298. [[CrossRef](#)]
19. Frazao, C.; Diaz, B.; Barros, J.; Bogas, J.A.; Toptan, F. An experimental study on the corrosion susceptibility of Recycled Steel Fibre Reinforced Concrete. *Cem. Concr. Compos.* **2019**, *96*, 138–153. [[CrossRef](#)]
20. Aiello, M.; Leuzzi, F.; Centonze, G.; Maffezzoli, A. Use of steel fibres recovered from waste tyres as reinforcement in concrete: Pull-out behaviour, compressive and flexural strength. *Waste Manag.* **2009**, *29*, 1960–1970. [[CrossRef](#)]
21. Zamanzadeh, Z.; Lourenço, L.; Barros, J. Recycled Steel Fibre Reinforced Concrete failing in bending and in shear. *Constr. Build. Mater.* **2015**, *85*, 195–207. [[CrossRef](#)]
22. Banthia, N.; Majdzadeh, F.; Wu, J.; Bindiganavile, V. Fiber synergy in Hybrid Fiber Reinforced Concrete (HyFRC) in flexure and direct shear. *Cem. Concr. Compos.* **2014**, *48*, 91–97. [[CrossRef](#)]
23. Liu, F.; Ding, W.; Qiao, Y. Experimental investigation on the tensile behavior of hybrid steel-PVA fiber reinforced concrete containing fly ash and slag powder. *Constr. Build. Mater.* **2020**, *241*, 118000. [[CrossRef](#)]
24. Dev, A.; Chellapandian, M.; Prakash, S.S.; Kawasaki, Y. Failure-mode analysis of macro-synthetic and hybrid fibre-reinforced concrete beams with GFRP bars using acoustic emission technique. *Constr. Build. Mater.* **2020**, *249*, 118737. [[CrossRef](#)]
25. Soltanzadeh, F.; Edalat-Behbahani, A.; Barros, J.A.O.; Mazaheripour, H. Effect of fibre dosage and prestress level on shear behavior of hybrid GFRP-steel reinforced concrete I-shape beams without stirrups. *Compos. Part B* **2016**, *102*, 57–77. [[CrossRef](#)]
26. Park, S.H.; Kim, D.J.; Ryu, G.S.; Koh, K.T. Tensile behavior of Ultra High Performance Hybrid Fiber Reinforced Concrete. *Cem. Concr. Compos.* **2012**, *34*, 172–184. [[CrossRef](#)]
27. Caggiano, A.; Folino, P.; Lima, C.; Martinelli, E.; Pepe, M. On the mechanical response of Hybrid Fiber Reinforced Concrete with Recycled and Industrial Steel Fibers. *Constr. Build. Mater.* **2017**, *147*, 286–295. [[CrossRef](#)]
28. Onuaguluchi, O.; Banthia, N. Scrap tire steel fibre as a substitute for commercial steel fibre in cement mortar: Engineering properties and cost-benefit analyses. *Resources. Conserv. Recycl.* **2018**, *134*, 248–256. [[CrossRef](#)]
29. Samarakoon, S.M.; Samindi, M.K.; Ruben, P.; Pedersen, J.W.; Evangelista, L. Mechanical performance of concrete made of steel fibres from tire waste. *J. Case Stud. Constr. Mater.* **2019**, *11*, e00259.
30. *BS EN 197-1 Cement; Composition, Specifications and Conformity Criteria for Common Cements*. BSI: London, UK, 2004. Available online: <http://www.rucem.ru/yabbfiles/Attachments/EN-197-1.pdf> (accessed on 20 January 2022).
31. Soltanzadeh, F.; Barros, J.A.O.; Santos, R.F.C. High performance fibre reinforced concrete for the shear reinforcement: Experimental and numerical research. *Constr. Build. Mater.* **2015**, *77*, 94–109. [[CrossRef](#)]
32. *BS EN 12350-8; Testing Fresh Concrete Self-Compacting Concrete. Slump-Flow Test*. European Standard: Pilsen, Czech Republic, 2019.
33. *BS EN 12390-13; Testing Hardened Concrete—Part 13: Determination of Secant Modulus of Elasticity in Compression*. European Standard: Pilsen, Czech Republic, 2014.
34. *ASTM C39/C39M-14a; Standard Test Method for Compressive Strength of Cylindrical Concrete Specimens*. Annual Book of ASTM Standards, American Society of Testing Materials: Washington, DC, USA, 2014.
35. RILEM TC 162-TDF. Bending test. *Mater. Struct.* **2002**, *35*, 579–582.
36. Soltanzadeh, F.; Cunha, V.M.C.F.; Barros, J.A.O. Assessment of different methods for characterization and simulation of post-cracking behavior of self-compacting steel fibre reinforced concrete. *Constr. Build. Mater.* **2019**, *227*, 116704. [[CrossRef](#)]
37. *ASTM C496; Standard Test Method for Splitting Tensile Strength of Cylindrical Concrete Specimens*. Annual Book of ASTM Standards, American Society of Testing Materials: Washington, DC, USA, 2004.
38. Caggiano, A.; Xargay, H.; Folino, P.; Martinelli, E. Experimental and numerical characterization of the bond behavior of steel fibres recovered from waste tires embedded in cementitious matrices. *Cem. Concr. Compos.* **2015**, *62*, 146–155. [[CrossRef](#)]
39. Soltanzadeh, F.; Behbahani, A.E.; Pereira, E.N.B.; Teixeira, C.A. A Life-Cycle Approach to Integrate Environmental and Mechanical Properties of Blended Cements Containing Seashell Powder. *Sustainability* **2021**, *13*, 13120. [[CrossRef](#)]
40. *ISO 14040; Environmental Management—Life Cycle 596 Assessment—Principles and Framework*. ISO: Geneva, Switzerland, 2006. Available online: <https://www.iso.org/standard/37456.html> (accessed on 20 January 2022).
41. *ISO 14044; Environmental Management—Life Cycle Assessment—Requirements and Guidelines*. ISO: Geneva, Switzerland, 2006. Available online: <https://www.iso.org/obp/ui/#iso:std:iso:14044:ed-1:v1:en> (accessed on 20 January 2022).
42. Hossain, M.U.; Ng, S.T. Critical consideration of buildings' environmental impact assessment towards adoption of circular economy: An analytical review. *J. Clean. Prod.* **2018**, *205*, 763–780. [[CrossRef](#)]
43. Xue, K.; Hossain, M.U.; Liu, M.; Ma, M.; Zhang, Y.; Hu, M.; Chen, X.; Cao, G. BIM Integrated LCA for Promoting Circular Economy towards Sustainable Construction: An Analytical Review. *Sustainability* **2021**, *13*, 1310. [[CrossRef](#)]
44. *Thinkstep GaBi Software, version 6.2*; ThinkStep: Leinfelden-Echterdingen, Germany, 2017.
45. Declaração Ambiental-SECIL-OUTÃO. SECIL—Companhia Geral de Cal e Cimento, S.A. 2019. Available online: <http://www.secil-group.com/wp-content/uploads/2020/11/V2004.012-DA2019-Maceira-signed.pdf> (accessed on 20 January 2022).
46. Fawer, M.; Concannon, M.; Rieber, W. Life cycle inventories for the production of sodium silicates. *Int. J. Life Cycle Assess.* **1999**, *4*, 207. Available online: <https://link.springer.com/content/pdf/10.1007/BF02979498.pdf> (accessed on 20 January 2022). [[CrossRef](#)]

47. Environmental Product Declaration Type III ITB No. 064/2017, Steel Fibres for Concrete Reinforcements. 2017. Available online: <https://www.itb.pl/g/f/2502,arcelormittal-sycow-wlokna-zbrojeniowe.pdf> (accessed on 15 September 2021).
48. Mateus, R.; Neiva, S.; Bragança, L.; Mendonça, P.; Macieira, M. Sustainability assessment of an innovative lightweight building technology for partition walls—Comparison with conventional technologies. *Build. Environ.* **2013**, *67*, 147–159. [[CrossRef](#)]
49. Guinée, J.B.; Gorrée, M.; Heijungs, R.; Huppes, G.; Kleijn, R.; de Koning, A.; van Oers, L.; Wegener Sleeswijk, A.; Suh, S.; Udo de Haes, H.A.; et al. Operational guide to the ISO standards. I: LCA in perspective. IIa: Guide. IIb: Operational annex. III: Scientific background. In *Handbook on Life Cycle Assessment*; Kluwer Academic Publishers: Dordrecht, The Netherlands, 2002; 692p, ISBN 1-4020-0228-9. Available online: <https://www.universiteitleiden.nl/en/research/research-projects/science/cml-new-dutch-lca-guide> (accessed on 20 January 2022).
50. Strange, A.; Park, J.; Bennett, R.; Phipps, R. The use of life-cycle assessment to evaluate the environmental impacts of growing genetically modified, nitrogen use-efficient canola. *Plant Biotechnol. J.* **2008**, *6*, 337–345. [[CrossRef](#)]
51. Siegl, S.; Laaber, M.; Holubar, P. Green Electricity from Biomass, Part I: Environmental Impacts of Direct Life Cycle Emissions. *Waste Biomass Valorization* **2011**, *2*, 267–284. [[CrossRef](#)]
52. Shi, J.; Li, T.; Zhang, H.; Peng, S.; Liu, Z.; Jiang, Q. Energy consumption and environmental emissions assessment of a re-frigeration compressor based on life cycle assessment methodology. *Int. J. Life Cycle Assess.* **2015**, *20*, 947–956. [[CrossRef](#)]
53. Teixeira, E.R.; Mateus, R.; Camões, A.; Bragança, L.; Branco, F.G. Comparative environmental life-cycle analysis of concretes using biomass and coal fly ashes as partial cement replacement material. *J. Clean. Prod.* **2016**, *112*, 2221–2230. [[CrossRef](#)]
54. Khodabakhshian, A.; de Brito, J.; Ghalehnovi, M.; Shamsabadi, E.A. Mechanical, environmental and economic performance of structural concrete containing silica fume and marble industry waste powder. *Constr. Build. Mater.* **2018**, *169*, 237–251. [[CrossRef](#)]
55. Li, S.; Jensen, O.M.; Yu, Q. Mechanism of rate dependent behaviour of ultra-high performance fibre reinforced concrete containing coarse aggregates under flexural loading. *Constr. Build. Mater.* **2021**, *301*, 124055. Available online: <https://www.sciencedirect.com/science/article/pii/S0950061821018158> (accessed on 20 January 2022). [[CrossRef](#)]
56. Edalat-Behbahani, A.; Barros, J.; Ventura-Gouveia, A. Plastic-damage smeared crack model to simulate the behaviour of structures made by cement based materials. *Int. J. Solids Struct.* **2015**, *73–74*, 20–40. [[CrossRef](#)]
57. Edalat-Behbahani, A.; Barros, J.; Ventura-Gouveia, A. Application of plastic-damage multidirectional fixed smeared crack model in analysis of RC structures. *Eng. Struct.* **2016**, *125*, 374–391. [[CrossRef](#)]
58. Edalat-Behbahani, A.; Barros, J.; Ventura-Gouveia, A. Three dimensional plastic-damage multidirectional fixed smeared crack approach for modelling concrete structures. *Int. J. Solids Struct.* **2017**, *115–116*, 104–125. [[CrossRef](#)]